CONF-901025--33

DE91 005488

High performance H modes in JET

The JET Team

(presented by A.Tanga)

JET Joint Undertaking, Abingdon, Oxon OX14 3EA, UK.

Abstract

In JET the scientific properties and technical basis of good confinement regimes have been evaluated in the light of the potential extrapolation of such regimes to reactor requirements. In this paper the main experimental H-mode results are discussed highlighting global confinement scaling, low q regimes, the role of the target plate material, the density limit, and finally sawtooth suppression and hot-ion mode.

1. Introduction

The H-mode in JET has been demonstrated with single and double null x-point configurations, which in general are marginally limiting at the x-point target tiles. H-modes have been achieved with NB heating, ICRF heating and with combined NB and ICRF heating. The power threshold for the H-mode and the global energy confinement time does not depend on the heating method. In the ELM free H-mode there is an improvement of about a factor of two in the global confinement time compared to JET limiter L-modes, up to the total additional power of 25MW.

The development of the JET H-mode, towards steady state conditions, depends on wall conditioning and on the material of the divertor target plates, which determines the amount and type of impurity released, and affect the time evolution of plasma density. The substantial reduction of Z_{eff} ($\simeq 2.$) and improvement of n_D/n_e to 0.8-0.9, produced by routine Beryllium gettering of the graphite tiles was probably mainly due to the nearly complete removal of Oxygen and Oxygen generated Carbon sputtering. The reduction of Nickel was mainly due to the Beryllium gettering of the ICRF antennae screens. As a consequence of lower radiation losses and improved density control longer ELM free H-mode phases have been achieved ($\lesssim 5.4$s) .

The transport of impurities in the JET H-mode is characterized by a balance between neoclassical effects and anomalous transport leading to a build up of impurities in the plasma ($\tau_{imp}/\tau_E > 1$) [1]. Further local analysis of energy transport in high power H modes confirms the reduction in thermal conductivity (energy flux.gradT) across the whole plasma cross section reported earlier [2] .

In the JET H-mode the density limit corresponds to the radiative collapse which ends the H phase.

With additional power well above the threshold, the H-mode can occur simultaneously with other plasma regimes such as the monster sawtooth or the hot-ion mode.

In the hot-ion H-mode, with NB(D)injection, at moderate plasma densities ($< n > 1 \div 4.10^{19}$ m^{-3}) T_i is 2 or 3 times larger than T_e ($T_i \gtrsim 22$keV, $Q_{dd} \simeq 2.5 \times 10^{-3}$). The values of Q_{DT} for D-T simulated versions of the same discharges are above 0.5 for times of the order of one energy confinement time.

2. Operational regimes

The H-mode in JET has been demonstrated in single null ($I_p < 5$MA) and double null ($I_p < 4.5$MA) configurations , generally with the plasma limiting on the x-point target tiles , but also with the plasma in contact with the inner wall. In single null configuration the H-mode has been achieved with NB at 80keV and at 140keV both in deuterium and hydrogen target plasmas. In double null configuration, where it has been possible to obtain good RF coupling, the H-mode has been achieved with ICRF alone in dipole with Hydrogen minority, and in combination with NB(D) in Deuterium plasmas. The JET H-mode is characterized by a transition to an ELM free period lasting several seconds. The duration of the H-mode is considerably shorter for power in excess of 10MW due to a strong carbon influx from overheated graphite dump tiles [3] .

The threshold power for the H-mode was similar for double and single null configurations, with ICRF and NB heating. The H-mode power threshold was lower with a well conditioned vessel. The power threshold, while scaling approximately linearly with the applied toroidal field as reported earlier [4], does not show a clear dependence on plasma current or plasma density. Scans of the plasma radial position show a minimum power threshold if the gap between the plasma and limiter, or between the plasma and the inner wall is above 5-8cm. For shorter distances the threshold power increases. H-mode was achieved even with the plasma in contact with the inner wall protection tiles, which required a threshold power of 10 MW at $B_T = 2.2$T. Plasma recycling and power load were distributed on the inner wall. We think that this regime is similar to the inner wall H-mode achieved in DIII-D [5] . Fig 1. shows the plot of additional heating power versus the gap between the plasma and the inner wall. L marks the discharges which had not undergone an H transition, while H marks the H modes. The H-mode power threshold is a function also of the position of the x-point as determined from magnetic diagnostics [6] . The threshold for H-mode has only a weak dependece on the location of the x-point within 10 cm outside the surface of the dump plate, with the plasma in a marginal limiter configuration or 10 cm inside, with plasma in x-point configuration.

3. Global confinement

The main properties of global confinement time of the JET H-mode have been extended to higher additional power. The general trend of the global energy confinement time, as a function of the total loss power, is shown in fig 2. The two main trends of increase with plasma current and degradation with heating power continue at high powers the trend reported earlier [4] . The scaling of the global confinement time is similar in single null and double null configuration. From the analysis the data it appears that the global confinement time has only a weak dependence on the toroidal field (as $B_T^{0.3\div0.07}$). In operation at low values $q_{0.95}$ it appeared that there was not an abroupt deterioration of confinement in the approach to $q_{0.95}$ of 2, as shown in fig 3. [7]. The scaling of the global confinement time observed in the JET H-mode is similar to that observed in other tokamaks. A size scaling has been derived by combining data from JET and DIII-D [8]. A large database with data from JET, DIII-D, ASDEX, JFT2-M, PDX and PBX has been created, the scaling obtained by the analysis of the data of all these tokamak is $\tau_E = 0.07 A^{.5} I^{.94} P^{-.48} R^{1.72} k^{0.48} (R/a)^{-0.13}$, when the toroidal field and density dependence are suppressed [9]. As an example a plot of the JET data versus the combined H-mode scaling, is shown in fig. 4. A detailed analysis of the local transport of JET H-mode will also be presented at this conferece [10].

4 Approach to steady state conditions

The ELM free H-mode is a transient effect which is terminated either by radiative collapse, for additional input power below 10MW, [11]; or by carbon influx, for power in excess of 10MW.

4.1 Carbon Influx

A strong carbon influx, which terminates the H-mode, enter the plasma when the surface temperature of the dump plates exceeds the temperature of 2500 C. The onset of the carbon influx can be delayed by radial sweeping of the x-point position or and by a strong gas puff. With strong puff long ELM free H-modes phases have been obtained, exceeding 5 seconds as shown in fig 5(a,b) The main effect of strong gas puff is a reduction of the surface temperature of the x-point tiles (fig 5 c,d) in the heated zone where the power is deposited by fast ions on drift orbits. [3,6] . The reduction in temperature is probably caused by reduced ion temperature and/or increased ion collisionality. The reduction in temperature leads to a significant drop in carbon sublimation and radiation enhanced sputtering. The gas puff causes increased divertor radiation losses with general reduction in conduction losses.

4.2 Radiative collapse.

The impurity confinement time, as determined by laser blow off measurements and impurities transport computer simulation [12] is much longer than the energy confinement time, with typical values up to 4s. [1,12] As an example the time evolution of the concentration of NickelXXV and NickelXXVI, obtained by laser blow-off of a Nickel coated target, are shown in fig 6. the result of transport analysis show that there is an outward flow of impurities, [1,12] . The plasma behaves as a " leaky " integrator. For intrinsic impurities, in the H-mode, the outward flow is an order of magnitude smaller than the inward flow, which is generated by the plasma interaction with the dump plates. Consequently, during the ELM free H-mode the concentration of the intrinsic

impurities increases continously as a function of time, until the total radiated power becomes excessive [11] . However if the inflow of intrinsic impurities could be reduced by at least a facor of 5, by for example the use of a pump divertor, the simulations show that a balance could be reached after a few impurity confinement times at levels of radiation compatible with the input power.

5. Effects of dump plate material on the H-mode.

The comparative properties of graphite and Beryllium gettered graphite have been studied.

With graphite tiles Oxygen and Carbon were the dominant impurities , radiative losses by Oxygen were dominant at high densities. Among other impurities Nickel, mainly generated by the ICFR antennae screens, accounted for a 10% fraction of the radiated power. With Beryllium gettered graphite tiles the concentration of Oxygen was reduced to a negligible amount. The reducion of Carbon concentration can be explained as due to the absence of Oxygen sputtering generated Carbon impurities as in the case of Beryllium gettered graphite limiter [13] .

In fig 7 the trend of Z_{eff} , as measured by visible bremsstrahlung, versus the total loss power (total input power minus the time derivative of the plasma energy) is shown. Fig 7 shows an average reduction of 1-2 units, at all levels of power. Consequently charge exchange spectroscopy measurements show that with Beryllium gettred graphite dump plates the ratio of electron to deuteron density was 0.8-0.9, whilst without Beryllium gettering it was 0.5-0.6.

6 Density limits

During the H-mode generally the plasma density increases continuosly until a radiative collapse of the H-mode occurs, [11] , precipitating an H to L transition and sometimes a full plasma disruption. For the H-mode the density limit coincides with the high density prior to the H to L transition. The limit on the plasma density is caused by the fact that the power which is radiated by the bulk of the plasma approaches the input power. It is therefore natural to expect the density limit to scale with the square root of the total input power with a scaling similar to that observed in in recent JET limiter discharges [14] . The values of the maximum volume average electron density prior to the H to L mode transition have been plotted versus the total input power in fig 8, for a series of 3MA H-mode discharges. the experimental points with Z_{eff} smaller than 3 (crosses) have a higer density than those with Z_{eff} larger than 3. For reference a Hugill plot of the non disrupting H-mode pulses is shown in fig 9 for discharges with Beryllium gettering.The line $qnR/B_t = 20x10^{19} m^{-2} T^{-1}$ encompasses the values for the dicharges with moderate additional heating (< 10MW) and fuelled by gas puffing. The lower limit $qnR/B_t = 12x10^{19} m^{-2} T^{-1}$ refers to Ohmic x-point

discharges. Preliminary results have been achieved with central pellet fueiling which have produced more peaked density profiles. The values of the pellet fuelled discharges are not shown in fig 9.

7. Sawtooth stabilization

Sawtooth suppression has been observed in H-mode discharges with NB and ICRF heating. The time evolution of a series of discharges showing sawtooth suppression during H-mode is presented in fig.10

With NB heating in excess of 8MW, at least twice the power threshold for H-mode transition, injected into a relatively low density ohmic deuterium target, the H-mode is accompained by a period of sawtooth stabilization of the duration of.6 -.8 s. In this phase a modest enhancement (10-15%) of central ion and electron temperatures is observed.

With ICRF heating during the H-mode [15] sawtooth suppression occurs routinely with ICRF input powers in excess of 7MW. The maximum duration of the monster sowtooth has been 2.5s. The start and end time of sawtooth suppression was not correlated with the H-mode phase, but sometimes the monster crash caused an H to L transition. The temperature peaking factor obtained in sawtooth suppressed H-modes is enhanced by approximately 50% . A series of electron temperature profile shapes with sawtooth suppressed H-modes is shown in fig 11. Here the peaking factor ranges between 3 and 4 (with electron pressure peaking factors between 4 and 5) with values of cylindrical $q = 3.2$ and averages densities in in the range $2 - 4 \times 10^{19} m^{-3}$. It should be noted that in this case the shape of the electron temperature profiles are similar to those obtained in the case of limiter monsters [16] and that the value of the edge plasma temperature is not very high.

With combined ICRF/NB heating sawtooth suppresion in H-mode has also been achieved, as shown by one of the traces in fig 12. In this pulse, ($P_{RF} = 2$MW and $P_{NB} = 6$MW, $< n > = 2.5$E19m-3). Polarimetric analysis of the safety factor radial profile indicate that the central value of q is driven below unity in a way similar to other monster sawtooth, while estimates of the content of fast particles confirm the agreement with the theoretical expectations of sawtooth stabilization.

8. Hot-ion H-mode

In x-point configuration with NB injection in a low density ohmic target it has been possible to produce simultaneously a hot-ion plasma and an H-mode transition. This regime is characterzed by very high ion temperatures in excess of 20keV. while the electron temperature vas 8-10keV. For large values of NB power and low densities the ion temperature profile is very peaked : The ratio of central to volume average ion temperature reaches values of 4-5 .

The D-T performances of these pulses ara examined by considering the standard $n_D \tau_E T_i$ diagram. shown in fig 13. Here the Q curves are for parabolic profiles of density and temperature raised to the power 1/2 and 3/2 respectively. The Q curves are rather insensitive to the form of the profiles. The time evolution of plasma parameters for pulse 20981 are shown in fig 14.

The time behaviour of the pulse was simulated by the 1 1/2-d TRANSP code for the actual conditions of NB injection and background plasma. A good check on the consistency of this data is that of the predicted and measured neutron yeld. The D-T simulations are completed by rerunning the code with the same measured profiles and replacing the background deuterium plasma with a tritium or with a 50-50 D-T mixture. The results are shown in fig 15. Here the time evolution of the fusion power is shown in its components for the case of deuterium injection in a Tritium plasma. The NB power was 17MW, the time derivative of plasma stored energy was 8MW. With Q defined as follow $Q = P_{th-th}/(P - dW/dt) + (P_{b-th} + P_{bb})/P$, the peak value corresponds to Q=0.77 [17].

9. Conclusions

a) The experiments at JET have shown that the ELM free H-mode is a transient plasma regime. The analysis of the results of impurities injection experiment and of the spectroscopical data suggests that if one could control the plasma density and drastically reduce the influx of impurities the H-mode could reach a steady state transport equilibrium.

b) The H-mode is achieved in a configuration with a magnetic separatrix, which can be marginally limiting on the x-point dump plates or on the inner wall protection plates. A parameter related to the shear at the plasma edge, for this marginally limiting configurations, could be the ratio between q_ψ and q_{cyl}. H-mode has been achieved with q_ψ larger or equal to 7-8 while q_{cyl} was 2-3.

c) In the H-mode the global energy confinement time shows an improvement of approximately a factor of two over the limiter L-mode independently of the heating method and in the range of additional power up to 25MW.

d)The radiation collapse, which terminates the H-mode, determines the values of the density limit, which scales with square root of the input power.

e) An improvement in plasma purity and reduction of fuel dilution has been achieved with Beryllium gettering of graphite tiles.

f) In low density ohmic target, and largely with ICRF heating it as been possible to achieve transient stabilization of sawteeth during the H-mode

g) With NB injection in low density deuterium plasmas a hot-ion plasma has been created during the H-mode. In these discharges the highest plasma thermonuclear reactivities have been obtained.

References :

1) Giannella R. et al. in Proc. of 16th European Conference on Contr. Fusion and Plasma Phys., Venice, 1989 Vol. I p.209.

2) Watkins M.L. et al. Plasma Phys. and Contr. Fusion Vol 31, p. 1713, (1989).

3) Stork D., et al. Proceedings of 9th International Conference on Plasma Surface Interactions, 21-25 May 1990, Bournemouth,UK paper P 25.

4) Keilhaker M. for the JET Team, Proc. 12th Conference on Plasma Physics and Controlled Nuclear Fusion, 12-19 October 1988, Nice, France, Vol I p. 159.

5) Jackson G.L., et al., Bull. Am. Soc. Vol 33 p. 1963 (1988)

6) O'Brien D.P., et al., Proc. 17th EPS Conference on Controlled Fusion and Plasma Physics, 25-29 June 1990, Amsterdam, The Netherlands, Vol I p.251.

7) Lazzaro E., et al., "H-mode confinement at low q and high beta in JET " to be published in Nuclear Fusion.

8) Shissel D.P., De Boo J.C., et al., Tubbing B.J.D., et al. "H-mode Energy Confinement scaling from DII-D and JET Tokamaks" to be published in Nuclear Fusion

9) Cordey J.G., et al., at this conference paper IAEA-CN-53/F/3-19

10) Taroni A., Tibone F., et al., at this conference paper IAEA-CN-53/A/2-1

11) Tanga A., et al., Nucl. Fus. Vol 27, p. 1877 (1987).

12) Lauro-Taroni L., et al., in Proc. 17th EPS Conference on Controlled Fusion and Plasma Physics, 25-29 June 1990, Amsterdam, The Netherlands, Vol I p.247.

13) Thomas P.R. for the JET Team, "Results of JET operation with Beryllium", Proceedings of 9th International Conference on Plasma Surface Interactions, 21-25 May 1990, Bournemouth,UK paper I:01.

14) Gibson A. for the JET Team " Fusion relevant performances in JET ", invited paper 17th EPS Conference on Controlled Fusion and Plasma Physics, 25-29 June 1990, Amsterdam, The Netherlands, to be published on Plasma Physics and Controlled Fusion
and Smeulders P. for the JET Team, at this conference, paper IAEA-CN53/A-3-4.

15) Tubbing B.J.D., et al., Nucl. Fus. vol 29, p. 1953 (1989)

16) Campbell D.J., et al., Proc. 11th Conference on Plasma Physics and Controlled Nuclear Fusion, 13-20 November 1986, Kyoto, Japan, Vol I p. 441.

17) Stubberfield P.M., Balet B. and Cordey J.G., "Extrapolation of the high performances JET plasmas to D-T operation " to be publlished on Plasma Physics and Controlled Fusion.

Figure captions

1) Plot of power threshold for H-mode transition as a function of the gap between the plasma and the inner wall protection tiles, for a series of NB heated disharges. Plasma current was 3MA, Toroidal field 2.2T. The symbol H represents the discharges which made the transition, the symbol L represents those discharges which stayed in L-mode. In the H area there are some discharges which did not make the transition.

2) Global energy confinement time versus total loss power for all the 3MA and 4MA discharges with $(dW/dt)/P < 0.3$. The solid points refer to pellet fuelled discharges.

3) Global enegrgy confinement time as a function of the safety factor at 95% of the flux surfaces. The data refer to a set of 3MA discharges in deuterium with NB heating in a narrow power range around 9MW. The range of toroidal field is betwwen 1.2 and 2.4T.

4) Global energy confinement time as measured, versus H-mode scaling derived by combining data from JET, DIII-D, PDX, PBX, JFT2-M.

5) Comparison of long pulse H-mode (pulse 21022) with (a) added gas, and (b) a discharge with same plasma and similar NB power with no added gas. The early carbon influx in the no gas shot can be clearly seen.in (c) and (d) the measured surface maximum temperature of the dump plate carbon tiles for the discharges in (a) and (b) respectively.

7) Comparison of the values of Z_{eff} from horizontal bremsstrahlung betwwen Carbon and Beryllium gettering for 3MA H-modes.

8) Volume average electron density at the end of 3MA H-mode pulses versus total input pover. The crosses refer to pulses with Z_{eff} less than 3.0 , while the squares refer to pulses with Z larger than 3.0. The line is $n_e(10^{19}m^{-3}) = 2.12 \times P^{0.5}(MW)$

9) Hugill plot for ohmic and additionally heated x-point discharges. Symbols: diamonds represent ohmically heated plasmas, crosses represent Neutral Beam heated plasmas, asterisks represent combined ICRF and NB heated plasmas.

10) Time evolution of central electron temperature in H-modes with suppressed sawtooth: pulse no.14834 NB heating, pulse no. 19797 NB/ICRF, pulses no.19995 and no.20231 ICRF heating.

11) LIDAR electron temperature profiles of H-mode with suppressed sawtooth, 1. pulse no. 20231, 3. pulse no. 19995, 4. pulse no. 19796, 2. limiter comparison case pulse no. 12924

12) Time evolution of ion and electron temperature for a sawtooth suppressed H-mode with combined ICRF and NB heating

13) $n_D \tau_E T_i$ versus $T_i(0)$

14) Time evolution of high fusion yeld pulse no 20981. from top to bottom are depicted the central ion temperature T_i , the total neutron yeld Y_n the plasma diamagnetic energy W_{dia} , the volume average electron density n_e , and D_α intensity near the x-point, the neutral beam power and the radiated power loss

as a function of time. The carbon influx at 11.5 s is followed by the loss of the H-mode.

15) TRANSP code simulation of a D-T version of pulse no. 20981 obtained by using the same set of the experimental measurements which are a good representation of the D-D case . The only changes are the species mix and the injection energy. This figure shows total fusion power, thermal and beam-thermal contributions, assuming 15MW of D (at 140keV) injection on a target Tritium plasma. Only D-T reactions have been considered.

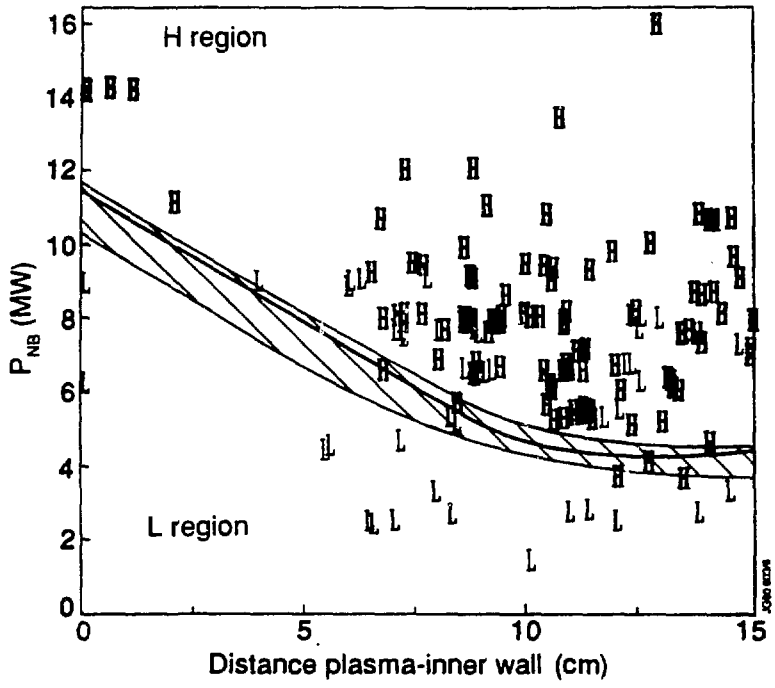

1) Plot of power threshold for H-mode transition as a function of the gap between the plasma and the inner wall protection tiles, for a series of NB heated disharges. Plasma current was 3MA, Toroidal field 2.2T. The symbol H represents the discharges which made the transition, the symbol L represents those discharges which stayed in L-mode. In the H area there are some discharges which did not make the transition.

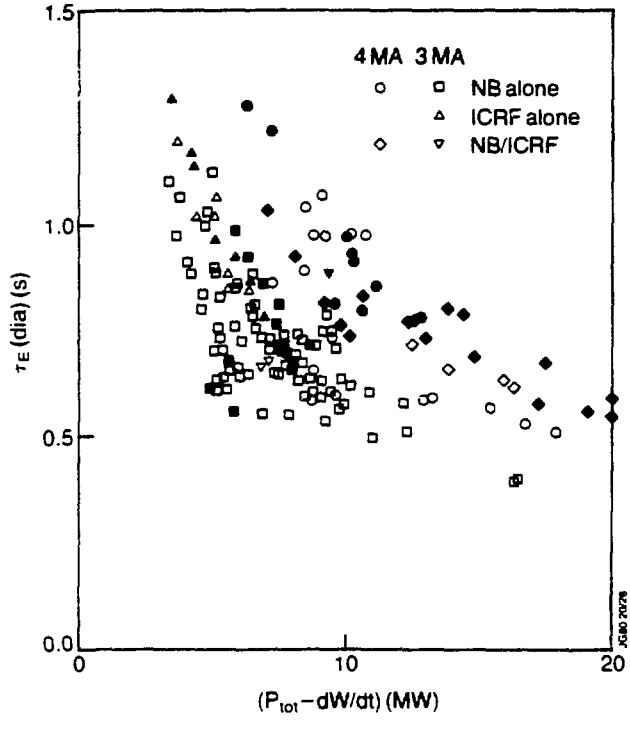

2) Global energy confinement time versus total loss power for all the 3MA and 4MA discharges with $(dW/dt)/P < 0.3$. The solid points refer to pellet fuelled discharges.

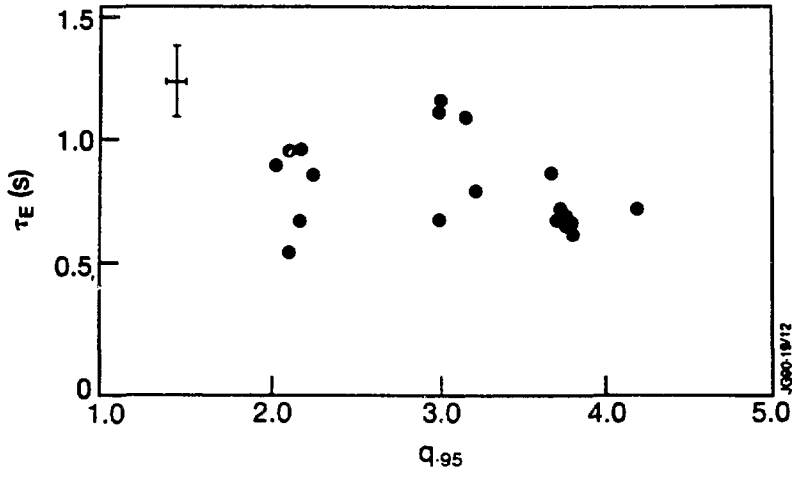

3) Global energy confinement time as a function of the safety factor at 95% of the flux surfaces. The data refer to a set of 3MA discharges in deuterium with NB heating in a narrow power range around 9MW. The range of toroidal field is betwwen 1.2 and 2.4T.

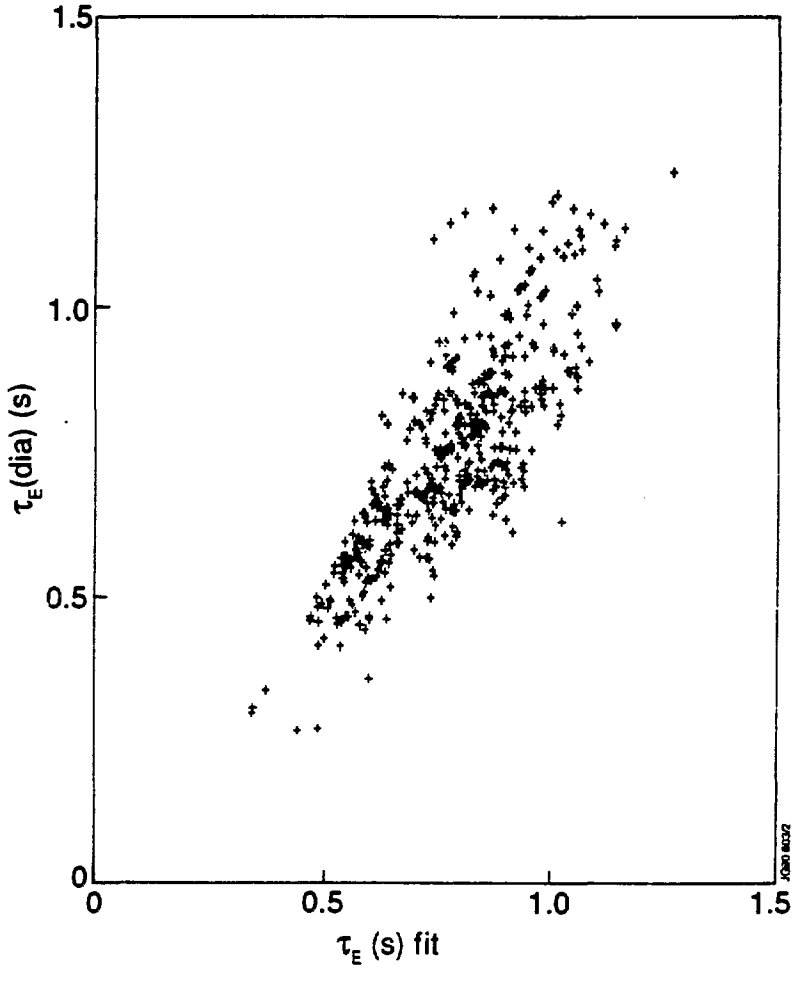

4) Global energy confinement time as measured, versus H-mode scaling derived by combining data from JET, DIII-D, PDX, PBX, JFT2-M.

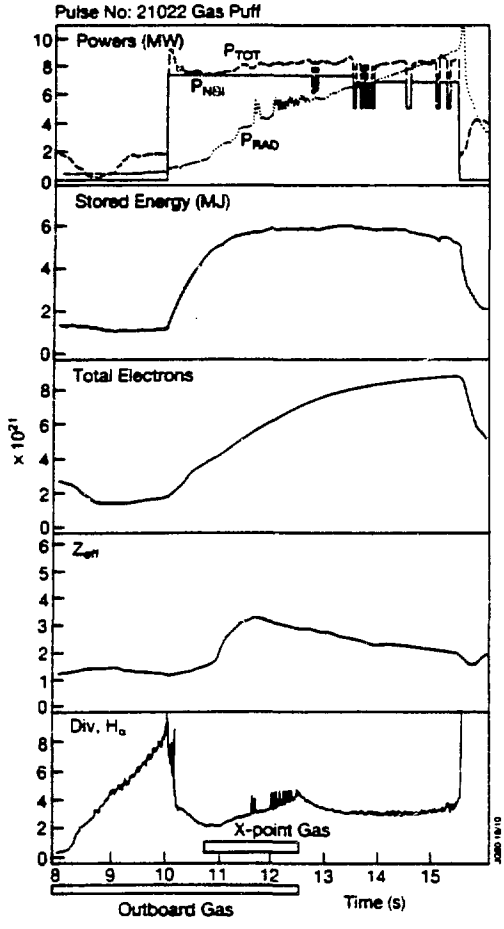

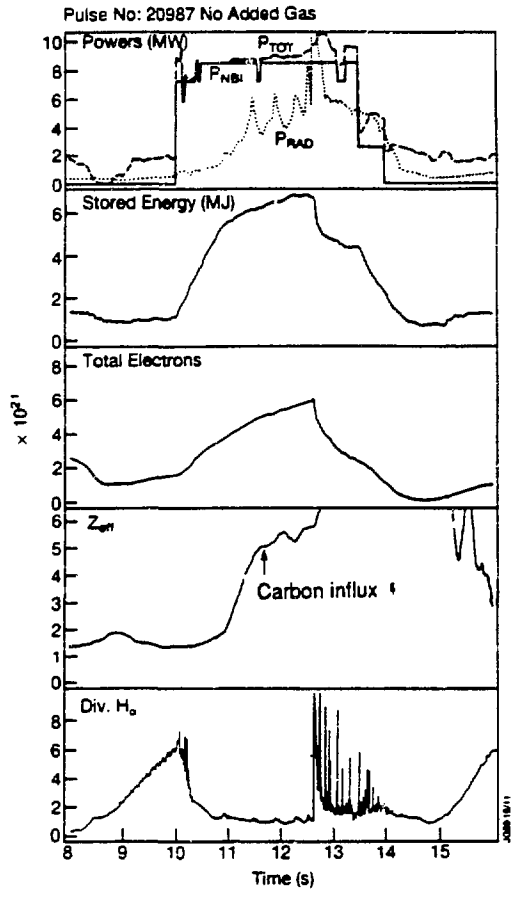

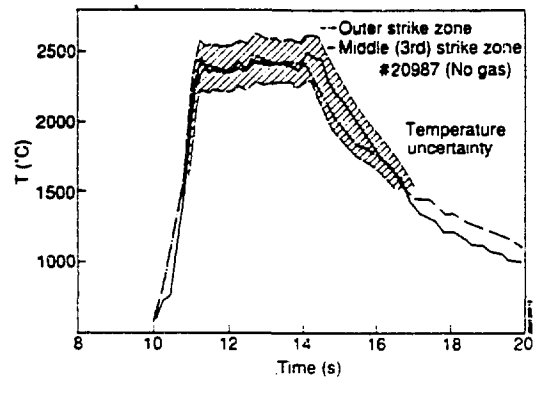

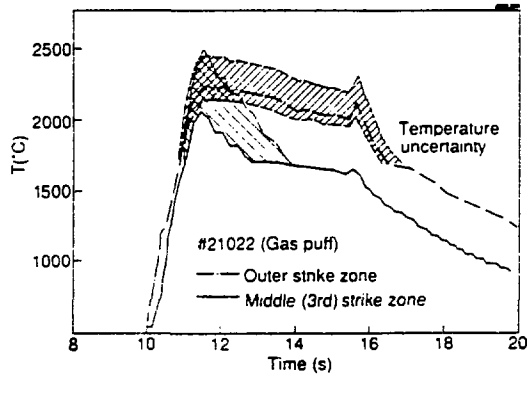

5) Comparison of long pulse H-mode (pulse 21022) with (a) added gas, and (b) a discharge with same plasma and similar NB power with no added gas. The early carbon influx in the no gas shot can be clearly seen in (c) and (d) the measured surface maximum temperature of the dump plate carbon tiles for the discharges in (a) and (b) respectively.

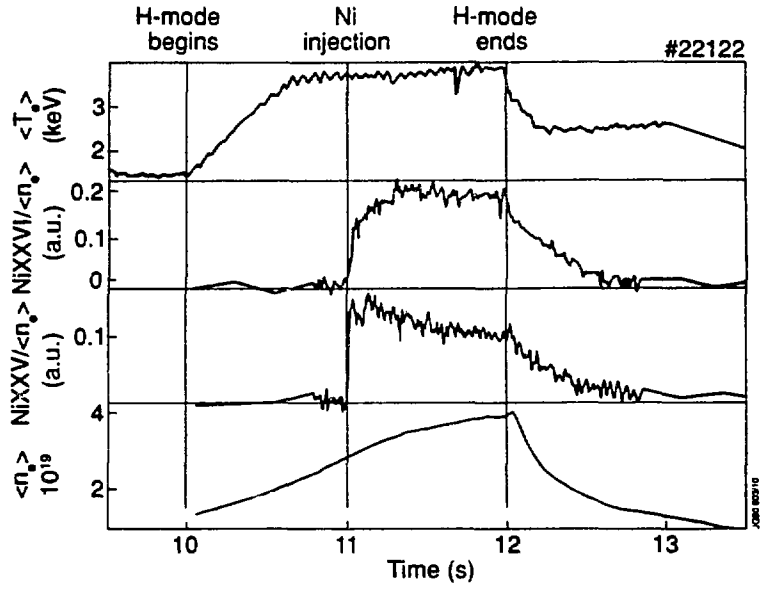

6) Time evolution of the ratio of the Nickel intensities during an H-mode. the Nickel is injected with laser blow-off tecnique at t = 11 s. Form top to bottom Volume average electron temperature, traces of density normalised NickelXXVI and NickelXXV, volume average plasma density.

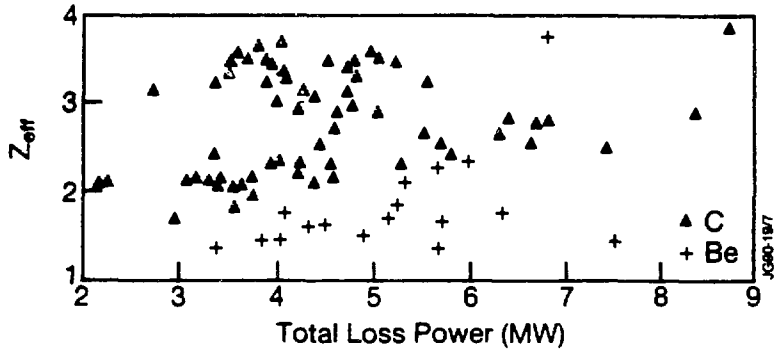

7) Comparison of the values of Z_{eff} from horizontal bremsstrahlung between Carbon and Beryllium gettering for 3MA H-modes.

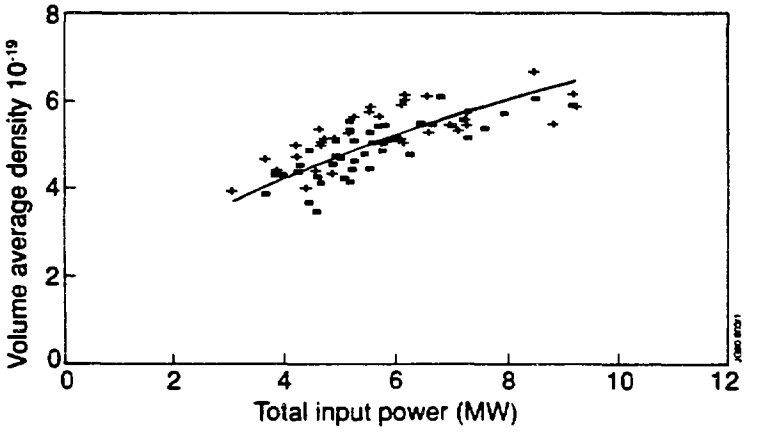

8) Volume average electron density at the end of 3MA H-mode pulses versus total input pover. The crosses refer to pulses with Z_{eff} less than 3.0 , while the squares refer to pulses with Z larger than 3.0. The line is $n_e(10^{19}m^{-3}) = 2.12 \times P^{0.5}(MW)$

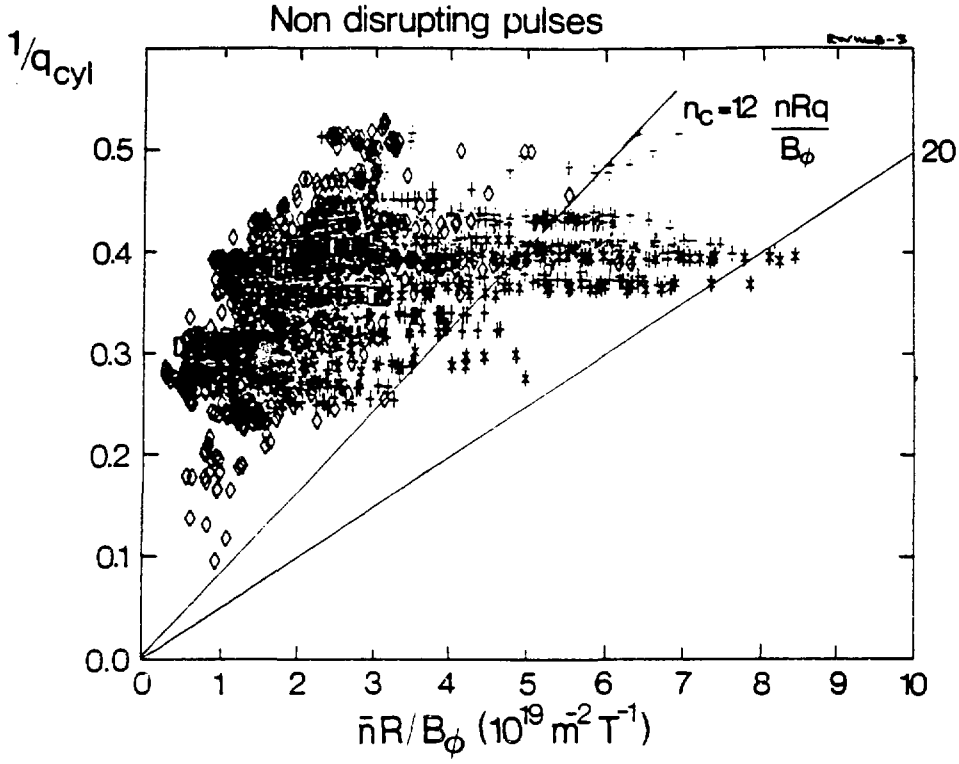

9) Hugill plot for ohmic and additionally heated x-point discharges. Symbols: diamonds represent ohmically heated plasmas, crosses represent Neutral Beam heated plasmas. asterisks represent combined ICRF and NB heated plasmas.

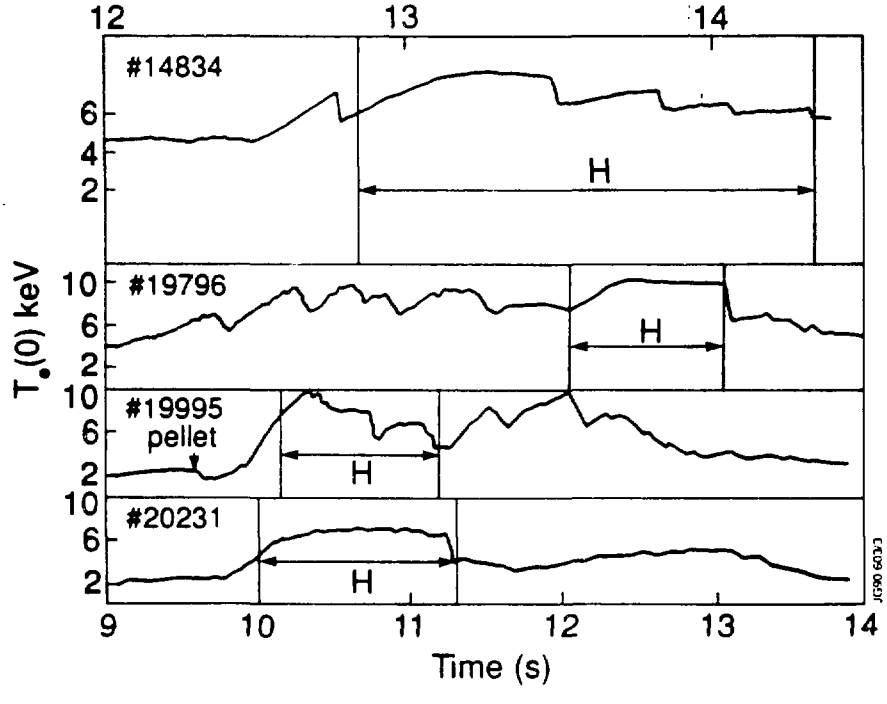

10) Time evolution of central electron temperature in H-modes with suppressed sawtooth: pulse no.14834 NB heating, pulse no. 19796 NB/ICRF, pulses no.19995 and no.20231 ICRF heating.

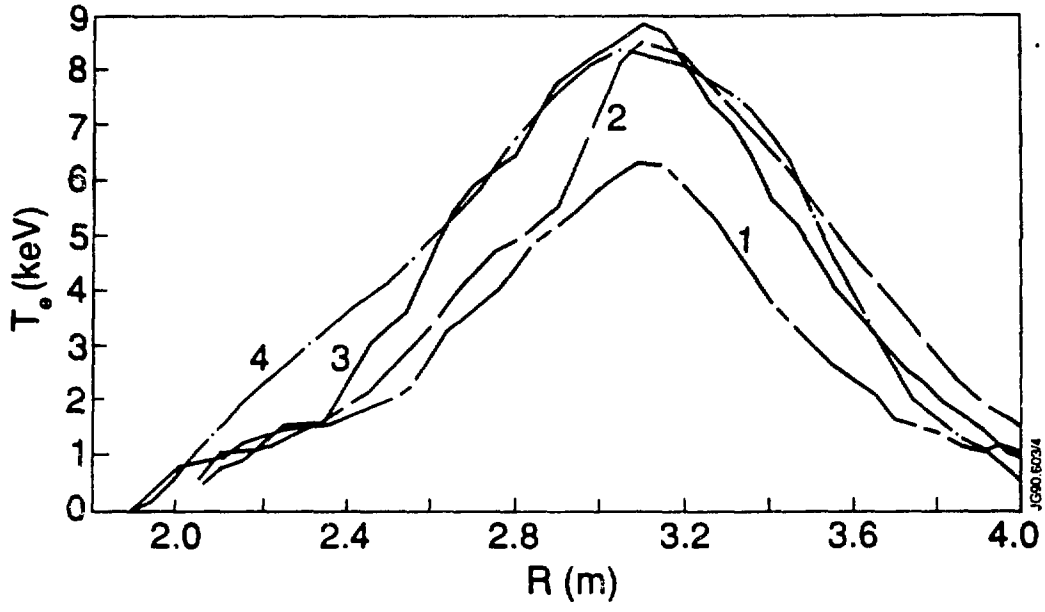

11) LIDAR electron temperature profiles of H-mode with suppressed sawtooth, 1. pulse no. 20231, 3. pulse no. 19995, 4. pulse no. 19796, 2. limiter comparison case pulse no. 12924

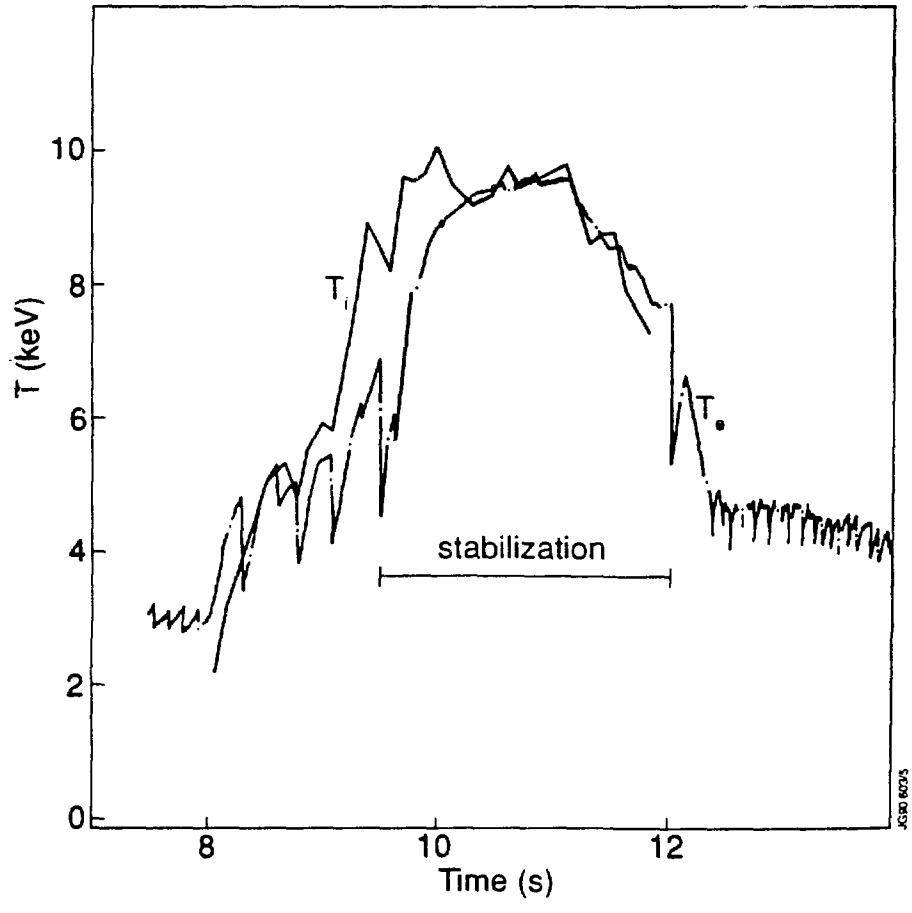

12) Time evolution of ion and electron temperature for a sawtooth suppressed H-mode with combined ICRF and NB heating

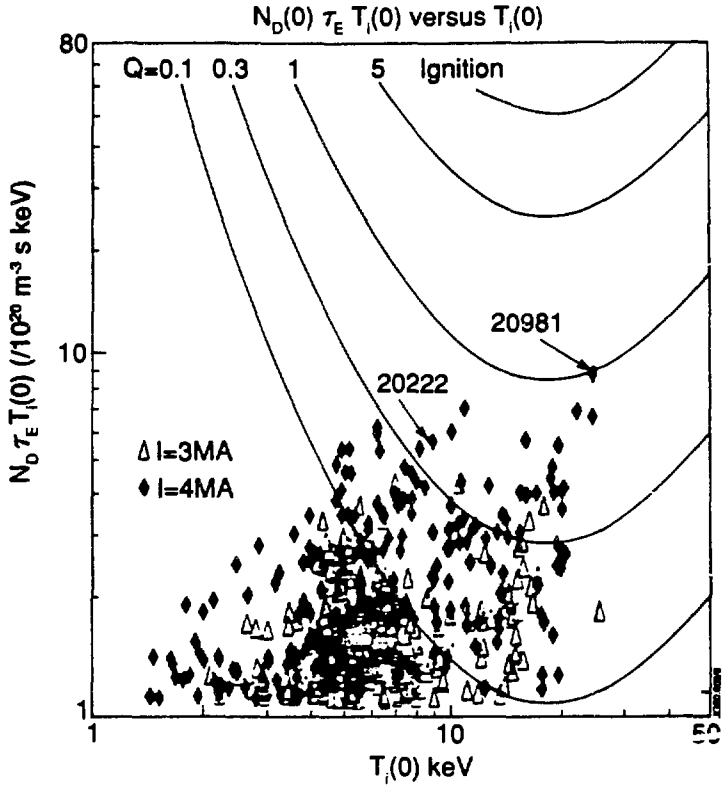

13) $n_D\tau_E T_i$ versus T_i (0)

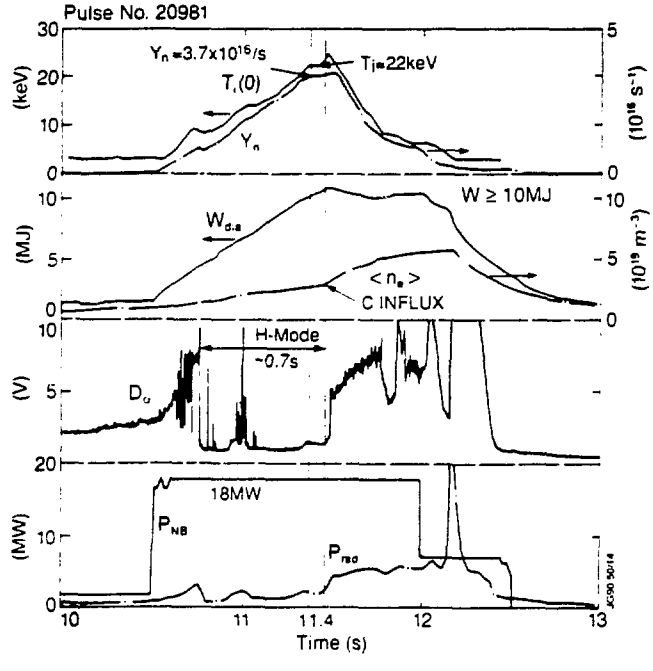

14) Time evolution of high fusion yeld pulse no 20981. from top to bottom are depicted the central ion temperature T_i , the total neutron yeld Y_n the plasma diamagnetic energy W_{dia} , the volume average electron density n_e , and D_α intensity near the x-point, the neutral beam power and the radiated power loss as a function of time. The carbon influx at 11.5 s is followed by the loss of the H-mode.

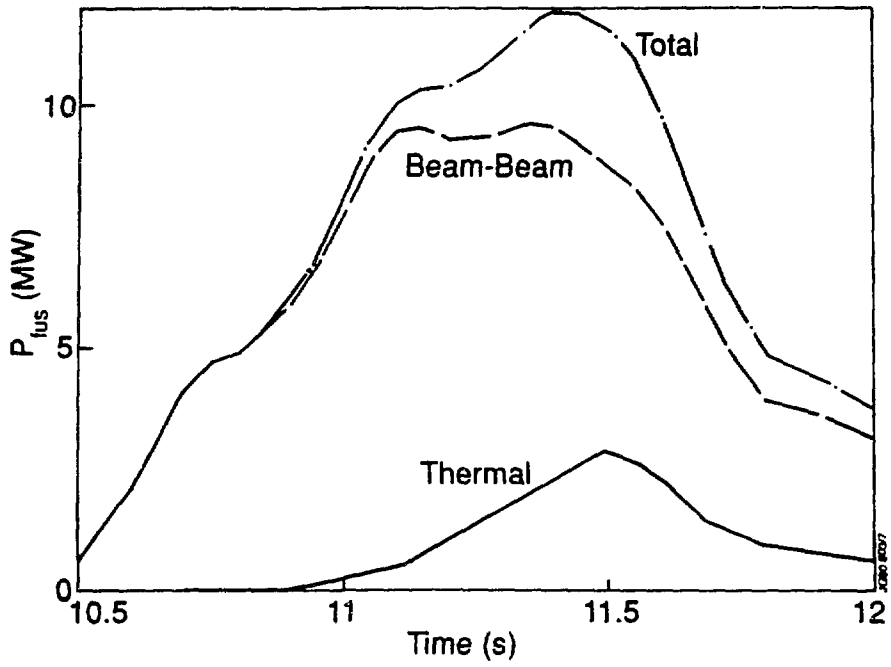

15) TRANSP code simulation of a D-T version of pulse no. 20981 obtained by using the same set of the experimental measurements which are a good representation of the D-D case . The only changes are the species mix and the injection energy. This figure shows total fusion power, thermal and beam-thermal contributions, assuming 15MW of D (at 140keV) injection on a target Tritium plasma. Only D-T reactions have been considered.